

---

# Learning Output Embeddings in Structured Prediction

---

**Luc Brogat-Motte**

Télécom Paris, IP Paris

luc.motte@telecom-paristech.fr

**Alessandro Rudi**

INRIA, ENS

alessandro.rudi@inria.fr

**Céline Brouard**

INRAE

celine.brouard@inrae.fr

**Juho Rousu**

Aalto University

juho.rousu@aalto.fi

**Florence d'Alché-Buc**

Télécom Paris, IP Paris

florence.dalche@telecom-paris.fr

## Abstract

A powerful and flexible approach to structured prediction consists in embedding the structured objects to be predicted into a feature space of possibly infinite dimension, and then, solving a regression problem in this output space. A prediction in the original space is computed by solving a pre-image problem. In such an approach, the embedding, linked to the target loss, is defined prior to the learning phase. In this work, we propose to jointly learn an approximation of the output embedding and the regression function into the new feature space. Output Embedding Learning (OEL) allows to leverage a priori information on the outputs and also unexploited unsupervised output data, which are both often available in structured prediction problems. We give a general learning method that we theoretically study in the linear case, proving consistency and excess-risk bound. OEL is tested on various structured prediction problems, showing its versatility and reveals to be especially useful when the training dataset is small compared to the complexity of the task.

## 1 Introduction

A large number of real-world applications involves the prediction of a structured output [28], whether it be a sparse multiple label vector in recommendation systems [39], a ranking over a finite number of objects in user preference prediction [16] or a labeled graph in metabolite identification [26]. Embedding-based methods generalizing ridge regression to structured outputs [40, 10, 3, 17, 5, 8], besides conditional generative models and margin-based methods [38, 37, 1], represent one of the main theoretical and practical frameworks to solve structured prediction problems and also find use in other fields of supervised learning such as zero-shot learning [30].

In this work, we focus on Output Kernel Regression (OKR) methods that rely on a simple idea: structured outputs are embedded into a Hilbert space, enabling to substitute to the initial structured output prediction problem, a less complex problem of vectorial output regression. Once this problem is solved, a structured prediction function is obtained by decoding the embedded prediction into the original output space, e.g. solving a pre-image problem. To benefit from an infinite dimensional embedding, the kernel trick can be leveraged in the output space, opening the approach to a large variety of structured outputs.

A generalization of the OKR approaches under the name of Implicit Loss Embedding has been recently studied from a statistical point of view in [9], extending the theoretical guarantees developed in [8, 27] about the Structure Encoding Loss Framework (SELF). In particular, it proved that the excess risk of the final structured output predictor depends on the excess risk of the surrogate regression estimator. This motivates the approach of this paper, controlling the error of the regression estimator by adapting the embedding to the observed data.

In this work, we propose to jointly learn a finite dimensional embedding that approximates the given embedding  $\psi$  and regress the new embedded output variable instead of the original embedding. Our contributions are four-fold:

- We introduce, Output Embedding Learning (OEL), a novel approach to Structured Prediction that jointly learns the embedding of outputs and the regression of the embedded output given the input, leveraging the prior information about the structure and unlabeled output data.
- We devise an OEL algorithm focusing on kernel ridge regression and a projection-based embedding that exploits the closed-form of the regression problem. We provide an efficient algorithm based on randomized SVD and Nyström approximation of kernel ridge regression.
- We derive excess risk bounds for this novel estimator, showing the relevance of this approach.
- We provide a comprehensive experimental study on various Structured Prediction problems with a comparison with dedicated methods, showing the versatility of our approach and highlighting the benefits of our approach when the training dataset size is small compared to the complexity of the task or when unlabeled data are available.

## 2 Output Embedding Learning

**Notations:**  $\mathcal{X}$  denotes the input space and  $\mathcal{Y}$  is the set of structured objects of finite cardinality  $|\mathcal{Y}| = D$ . Given two spaces  $\mathcal{A}, \mathcal{B}$ ,  $\mathcal{F}(\mathcal{A}, \mathcal{B})$  denotes the set of functions from  $\mathcal{A}$  to  $\mathcal{B}$ . Given two Hilbert spaces  $\mathcal{H}_1$  and  $\mathcal{H}_2$ ,  $\mathcal{B}(\mathcal{H}_1, \mathcal{H}_2)$  is the space of bounded linear operators from  $\mathcal{H}_1$  to  $\mathcal{H}_2$ .  $Id_{\mathcal{H}_1}$  is the identity operator over  $\mathcal{H}_1$ . The adjoint of an operator  $A$  is noted  $A^*$ .

Structured Prediction is generally associated to a loss  $\Delta : \mathcal{Y} \times \mathcal{Y} \rightarrow \mathbb{R}$  that takes into account the inherent structure of objects in  $\mathcal{Y}$ . In this work, we consider a structure-dependent loss by relying on an embedding  $\psi : \mathcal{Y} \rightarrow \mathcal{H}_y$  that maps the structured objects into a Hilbert space  $\mathcal{H}_y$  and the squared loss defined over pairs of elements of  $\mathcal{H}_y$ :  $\Delta(y, y') = \|\psi(y) - \psi(y')\|_{\mathcal{H}_y}^2$ .

A principled and general way to define the embedding  $\psi$  consists in choosing  $\psi(y) = k(\cdot, y)$ , the canonical feature map of a positive definite symmetric kernel  $k$  defined over  $\mathcal{Y}$ , referred here as the *output kernel*. The space  $\mathcal{H}_y$  is then the Reproducing Kernel Hilbert Space associated to kernel  $k$ . This choice enables to solve various structured prediction problems within the same setting, drawing on the rich kernel literature devoted to structured objects [12].

Given an unknown joint probability distribution  $P(X, Y)$  defined on  $\mathcal{X} \times \mathcal{Y}$ , the goal of structured prediction is to solve the following learning problem:

$$\min_{f \in \mathcal{F}(\mathcal{X}, \mathcal{Y})} \mathbb{E}_{X, Y \sim P} \left[ \|\psi(Y) - \psi(f(X))\|_{\mathcal{H}_y}^2 \right], \quad (1)$$

with the help of a training i.i.d. sample  $\mathcal{S}_n = \{(x_i, y_i), i = 1, \dots, n\}$  drawn from  $P$ .

To overcome the inherent difficulty to learn  $f$  through  $\psi$ , embedding-based approaches address structured prediction by solving the Output Kernel Regression as a surrogate problem, e.g. regressing the target variable  $\psi(Y)$  given  $X$ , and then make their prediction in the original space  $\mathcal{Y}$  with a decoding function as follows (see Figure 1, left):

$$h_\psi^* \in \arg \min_{h \in \mathcal{F}(\mathcal{X}, \mathcal{H}_y)} \mathbb{E}_{X, Y \sim P} \left[ \|\psi(Y) - h(X)\|_{\mathcal{H}_y}^2 \right], \quad (2)$$

This regression step is then followed by a pre-image or *decoding* step in order to recover  $f^*$ :

$$f^*(x) = d \circ h^*(x),$$

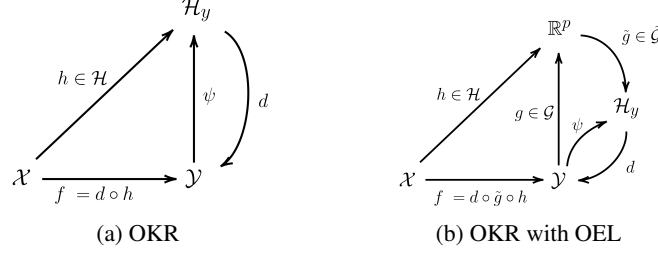


Figure 1: Schematic illustration of OKR and OKR with OEL

where the decoding function  $d$  computes  $d(z) = \arg \min_{y \in \mathcal{Y}} \|\hat{h}(x) - \psi(y)\|_{\mathcal{H}_y}^2$ .

While the above is a powerful approach for structured prediction, relying on a fixed output embedding given by  $\psi$  may not be optimal in terms of prediction error, and it is hard by a human expert to decide on a good embedding.

In this paper, we propose to jointly learn a novel output embedding  $g : \mathcal{Y} \rightarrow \mathbb{R}^p$  as a finite dimensional proxy of  $\psi$  and the corresponding regression model  $h : \mathcal{X} \rightarrow \mathbb{R}^p$ .

Our novel approach, called Output Embedding Learning (OEL), thus consists in solving the two problems (Figure 1, right).

**Learning:** for a given hyperparameter  $\gamma$ ,

$$(h^*, g^*, \tilde{g}^*) \in \arg \min_{h, g, \tilde{g}} \gamma \underbrace{\mathbb{E}_{X, Y} [\|h(X) - g(Y)\|_{\mathbb{R}^p}^2]}_{\mathcal{L}(h, g)} + (1 - \gamma) \underbrace{\mathbb{E}_Y [\|\tilde{g} \circ g(Y) - \psi(Y)\|_{\mathcal{H}_y}^2]}_{\Gamma(g)}, \quad (3)$$

**Decoding:**

$$f^*(x) = d \circ \tilde{g}^* \circ h_{g^*}^*(x), \quad (4)$$

where the decoding output is  $d(z) = \arg \min_{y \in \mathcal{Y}} \|\psi(y) - z\|_{\mathcal{H}_y}^2$ .

In the learning objective of Eq. (3), the term  $\mathcal{L}(h, g)$  expresses a surrogate regression problem from the input space to the learned output embedding space while  $\Gamma(g)$  is a reconstruction error that constrains  $g$  to provide a good proxy of  $\psi$ , and thus, encouraging the novel surrogate loss  $(h(x), y) \rightarrow \|h(x) - g(y)\|^2$  to be calibrated with loss  $\Delta$ .

This approach allows learning an output embedding that, intuitively, is easier to predict from inputs than  $\psi$  and also provides control of the complexity of surrogate regression model  $h$  by choosing the dimension  $p$ .

To solve the learning problem in practise, a training i.i.d. sample  $\mathcal{S}_n = \{(x_i, y_i), i = 1, \dots, n\}$  is used for estimating  $\mathcal{L}(h, g)$ . For estimating  $\Gamma(g)$  we can also benefit from additional i.i.d. samples of the outputs  $Y$ , denoted  $\mathcal{U}_m$ . Such data is generally easy to obtain for many structured output problems, including the metabolite identification task described in the experiments.

## 2.1 Solving OEL with a linear transformation of the embedding

We consider the case where the chosen model for the output embedding is a linear transformation of  $\psi$ :  $g(y) = G\psi(y)$  where  $G$  is an operator,  $G \in \mathcal{G}_p = \{A \in \mathcal{L}(\mathcal{H}_y, \mathbb{R}^p), AA^* = Id_p\}$ , with the linear associated decodings:  $\tilde{g}(z) = G^*z \in \mathbb{R}^p$ . Here  $\tilde{g} \circ g$  can be interpreted as a one-layer linear autoencoder whose inputs and outputs belong to the Hilbert space  $\mathcal{H}_y$  (thus giving overall non-linear embedding  $g$ ) [20], and the hidden layer is trained in supervised mode (through  $h$ ), or alternatively as a Kernel PCA model [34] of the outputs, but trained in supervised mode.

We denote  $h_\psi^*(x)$  the conditional expectation of  $\psi(Y)$  given  $x$ ,  $h_\psi^*(x) = \mathbb{E}_y[\psi(y)|x]$ . Within this setting, the general problem depicted in Eq. 3 instantiates as follows:

$$\min_{h \in \mathcal{F}(\mathcal{X}, \mathbb{R}^p), G \in \mathcal{G}_p} \gamma \mathbb{E}_{X, Y} [\|h(X) - G\psi(Y)\|_{\mathbb{R}^p}^2] + (1 - \gamma) \mathbb{E}_Y [\|G^*G\psi(Y) - \psi(Y)\|_{\mathcal{H}_y}^2]. \quad (5)$$

Leveraging the regression  $h_\psi^*(x)$ , and  $\|G\psi(y)\|_{\mathbb{R}^p} = \|G^*G\psi(y)\|_{\mathcal{H}_y}$  ( $G$  is orthogonal), this is equivalent to solve the following problem<sup>1</sup>:

$$\min_G \gamma \mathbb{E}_X[\|G^*Gh_\psi^*(X) - h_\psi^*(X)\|_{\mathcal{H}_y}^2] + (1 - 2\gamma)\mathbb{E}_Y[\|G^*G\psi(Y) - \psi(Y)\|_{\mathcal{H}_y}^2], \quad (6)$$

where we restrict  $\gamma \leq \frac{1}{2}$  to ensure the objective is theoretically grounded. In the following, we use  $\gamma_c := \frac{c}{1+c} \leq \frac{1}{2}$ , with  $c \in [0, 1]$ . The objective boils down to estimating the linear subspaces of the  $\mathbb{E}_{y|x}[\psi(y)]$  and the  $\psi(y)$ .

In the empirical context, given an i.i.d. labeled sample  $\{(x_i, y_i), i = 1, \dots, n\}$ , and an i.i.d unlabeled sample  $\{y_j, j = 1, \dots, m\}$ , we propose to use an empirical estimate  $\hat{h}_\psi$  of the unknown conditional expectation  $h_\psi^*$  and solve the following remaining optimization problem in  $G$ :

$$\min_{G \in \mathcal{G}_p} \frac{c}{n} \sum_{i=1}^n \|G^*G\hat{h}_\psi(x_i) - \hat{h}_\psi(x_i)\|_{\mathcal{H}_y}^2 + \frac{(1-c)}{m} \sum_{j=1}^m \|G^*G\psi(y_j) - \psi(y_j)\|_{\mathcal{H}_y}^2. \quad (7)$$

**Learning in vector-valued RKHS:** To find an empirical estimate of  $h_\psi^*$ , we need a hypothesis space  $\mathcal{H} \subset \mathcal{F}(\mathcal{X}, \mathcal{H}_y)$ , whose functions have infinite dimensional outputs. Following the Input Output Kernel Regression approach depicted in [5], we solve a kernel ridge regression problem in  $\mathcal{H}_K$ , the RKHS associated to the operator-valued kernel  $K(x, x') = Id_{\mathcal{H}_y} k_x(x, x')$  and we got the following closed-form expression:

$$\hat{h}_\psi(x) = \sum_{i=1}^n \alpha_i(x) \psi(y_i), \text{ with } \alpha(x) = (K_x + n\lambda I)^{-1} \kappa_X^x, \quad (8)$$

where  $\kappa_X^x = [k_x(x_1, x), \dots, k_x(x_n, x)]^T$  and  $\lambda > 0$  is the ridge regularization hyperparameter.

**OEL estimator:** For a given  $(c, \lambda, p)$ , denoting  $\hat{G}_p$  as the solution of the above convex problem, the proposed estimator for the solution of the problem stated in Eq. 5 can be expressed as:  $\hat{h}_{\hat{G}_p}(x) = \hat{G}_p \hat{h}_\psi(x)$ . However it is important to stress that we only need to compute the associated structured prediction function:

$$\hat{f}(x) = \arg \min_{y \in \mathcal{Y}} \|\hat{G}_p^* \hat{G}_p \hat{h}_\psi(x) - \psi(y)\|_{\mathcal{H}_y}^2 \quad (9)$$

$$= \arg \min_{y \in \mathcal{Y}} \|\hat{h}_{\hat{G}_p}(x) - \hat{G}_p \psi(y)\|_{\mathcal{H}_y}^2 + \|\hat{G}_p^* \hat{G}_p \psi(y) - \psi(y)\|_{\mathcal{H}_y}^2 \quad (10)$$

We derive Algorithm 1 which consists in computing the singular value decomposition of the mixed gram matrix  $K$ , noticing that the objective 7 is equivalent to minimize the empirical mean reconstruction error of the  $n + m$  vectors of  $\mathcal{H}_y$ :

$$\left( \sqrt{\frac{c}{n}} \hat{h}_\psi(x_1), \dots, \sqrt{\frac{c}{n}} \hat{h}_\psi(x_n), \sqrt{\frac{(1-c)}{m}} \psi(y_1), \dots, \sqrt{\frac{(1-c)}{m}} \psi(y_m) \right).$$


---

**Algorithm 1:** Output Embedding Learning with KRR (Training)

---

**Input:**  $K_x, K_y^{s,s} \in \mathbb{R}^{n \times n}$  (supervised data),  $K_y^{u,u} \in \mathbb{R}^{m \times m}, K_y^{s,u} \in \mathbb{R}^{n \times m}$  (unsupervised data),  $\lambda \geq 0$  KRR regularization,  $p \in \mathbb{N}^*$  embedding dimension,  $c \in [0, 1]$  supervised/unsupervised balance.

**IKRR estimation:**  $W = (K_x + n\lambda I)^{-1} / K_h = W K_x K_y^{s,s} K_x W / K_{hy} = W K_x K_y^{s,u}$

**ISubspace estimation:**

$$\begin{aligned} 1) \ K &= \begin{bmatrix} \frac{c}{n} K_h & \sqrt{\frac{c(1-c)}{nm}} K_{hy} \\ \sqrt{\frac{c(1-c)}{nm}} K_{hy}^T & \frac{(1-c)}{m} K_y^{u,u} \end{bmatrix} \in \mathbb{R}^{(n+m) \times (n+m)} \\ 2) \ \beta &= \begin{bmatrix} \frac{u_1}{\sqrt{\mu_1}} & \dots & \frac{u_p}{\sqrt{\mu_p}} \end{bmatrix} \in \mathbb{R}^{(m+n) \times p} \leftarrow SVD(K) = \sum_{l=1}^{n+m} \mu_l u_l u_l^T \\ 3) \ GY &= K\beta \end{aligned}$$

**return**  $W$  KRR coefficients,  $\beta$  output embedding coefficients,  $GY$  new training embedding

---

<sup>1</sup>see details in Section 1 of the supplements

**Computational complexity** The complexity in time of the training Algorithm 1 is the sum of the complexity of a Kernel Ridge Regression (KRR) with  $n$  data and a Singular Value Decomposition with  $n + m$  data:  $\mathcal{O}(n^3) + \mathcal{O}((n + m)^3)$ . However, this complexity can be a lot improved as for both KRR and SVD there exists a rich literature of approximation methods [33, 15]. For instance, using Nyström KRR approximation of rank  $q$  and randomized SVD approximation of rank  $p$ , then, the time complexity becomes:  $\mathcal{O}(nq^2 + q^3) + \mathcal{O}((n + m)^2p + (n + m)p^2)$ .

### 3 Theoretical analysis

From a statistical viewpoint we are interested in controlling the *expected risk* of the estimator  $f = d \circ \tilde{g} \circ h$ , that for the considered loss corresponds to

$$\mathcal{R}(f) = \mathbb{E}_{X,Y} [\|\psi(f(X)) - \psi(Y)\|_{\mathcal{H}_y}^2].$$

Interpreting the decoding step in the context of structured prediction, we can leverage the so called *comparison inequality* from [8]. This inequality is applied for our case in the next lemma and relates the excess-risk of  $f = d \circ \tilde{g} \circ h$  to the  $L^2$  distance of  $\tilde{g} \circ \hat{h}$  to  $h_\psi^*$  (see [8] for more details on structured prediction and the comparison inequality).

**Lemma 3.1.** *For every measurable  $\hat{h} : \mathcal{X} \rightarrow \mathbb{R}^p$ ,  $\tilde{g} : \mathbb{R}^p \rightarrow \mathcal{H}_y$ ,  $f = d \circ \tilde{g} \circ \hat{h}$ ,*

$$\mathcal{R}(f) - \mathcal{R}(f^*) \leq c(\psi) \sqrt{\mathbb{E}_X \|\tilde{g} \circ \hat{h}(X) - h_\psi^*(X)\|_{\mathcal{H}_y}^2}$$

with  $c(\psi) = 2\sqrt{2Q^2 + Q^4 + 1}$ ,  $Q = \sup_{y \in \mathcal{Y}} \|\psi(y)\|^2$ .

It is possible to apply the comparison inequality, since the considered loss function  $\Delta(y, y') = \|\psi(y) - \psi(y')\|_{\mathcal{H}_y}^2$  belongs to the wide family of SELF losses [8] for which the comparison inequality holds. A loss is SELF if it satisfies the *implicit embedding property* [9], i.e. there exists an Hilbert space  $\mathcal{V}$  and two feature maps  $\gamma, \theta : \mathcal{Y} \rightarrow \mathcal{V}$  such that

$$\Delta(y, y') = \langle \gamma(y), \theta(y') \rangle_{\mathcal{V}}, \quad \forall y, y' \in \mathcal{Y}.$$

In our case the construction is direct and corresponds to  $\mathcal{V} = \mathcal{H}_y \oplus \mathbb{R} \oplus \mathbb{R}$ ,  $\gamma(y) = (\sqrt{2}\psi(y), \|\psi(y)\|_{\mathcal{H}_y}^2, 1)$  and  $\theta(y') = (-\sqrt{2}\psi(y'), 1, \|\psi(y')\|_{\mathcal{H}_y}^2)$ .

Intuitively, the idea of output embedding learning, is to find a new embedding that provides an easier regression task while being still able to predict in the initial regression space. In our formulation this is possible due to introduction of  $\tilde{g}$  and a suitable choice of  $\mathcal{G}, \tilde{\mathcal{G}}$ . In this construction  $\tilde{g} \circ h$  can be decomposed into two parts:

$$\underbrace{\mathbb{E}_X [\|\tilde{g} \circ \hat{h}_g(X) - h_\psi^*(X)\|^2]}_{\text{initial regression problem}} = \underbrace{\mathbb{E}_X [\|\tilde{g} \circ \hat{h}_g(X) - \tilde{g} \circ h_g^*(X)\|^2]}_{\text{simplified regression problem}} + \underbrace{\mathbb{E}_X [\|\tilde{g} \circ h_g^*(X) - h_\psi^*(X)\|^2]}_{\text{reconstruction error}} \quad (11)$$

In the case of KRR, linear projections  $\tilde{g} : z \in \mathbb{R}^p \rightarrow \tilde{G}z \in \mathcal{H}_y$ , and arbitrary set of function  $\mathcal{G}$  from  $\mathbb{R}^p$  to  $\mathcal{H}_y$ , the left term expresses as KRR excess-risk on a linear subspace of  $\mathcal{H}_y$  of dimension  $p$ . For the right term, defining the covariance  $M_c : \mathcal{H}_y \rightarrow \mathcal{H}_y$  for all  $c \in [0, 1]$ ,

$$M_c = c\mathbb{E}_x(h^*(x) \otimes h^*(x)) + (1 - c)\mathbb{E}_y(\psi(y) \otimes \psi(y)) \quad (12)$$

we have the following bound due to Jensen inequality,

**Lemma 3.2.** *Under the assumptions of Lemma 3.1, when  $\tilde{g}$  is a linear projection, we have*

$$\mathbb{E}_x [\|\tilde{g}(h_g^*(x)) - h_\psi^*(x)\|^2] \leq \langle I - P, M_c \rangle_{\mathcal{H}_y \otimes \mathcal{H}_y}$$

The closer  $c$  is to 1, the tighter is the bound, but having  $c$  close to 0 could lead to a much easier learning objective. Relying on results on subspace learning in [32] and following their proofs, we bound this upper bound and get the Theorem 3.3. In particular, we use natural assumption on the spectral properties of the mixed covariance operator  $M_c$  as introduced in [32].

**Assumption 1.** *There exist  $\omega, \Omega > 0$  and  $r > 1$  such that the eigendecomposition of the positive operator  $M_c$  has the following form*

$$M_c = \sum_{j \in \mathbb{N}} \sigma_j u_j \otimes u_j, \quad \omega j^{-r} \leq \sigma_j \leq \Omega j^{-r}. \quad (13)$$

The assumption above controls the so called *degrees of freedom* of the learning problem. A fast decay of  $\sigma_j$  can be interpreted as a problem that is well approximated by just learning the first few eigenvectors (see [6, 32] for more details). To conclude, the first part of the r.h.s. of 11 is further decomposed and then bounded via Lemma 18 of [8], leading to Theorem 3.3. Before we need an assumption on the approximability of  $h_\psi^*$ .

**Assumption 2.** *The function  $h_\psi^*$  satisfies  $h_\psi^* \in \mathcal{H}_y \otimes \mathcal{H}_x$ .*

The assumption above where  $\mathcal{H}_x$  is the RKHS associated to  $k_x$ , guarantees that  $h_\psi^*$  is approximable by kernel ridge regression with the given choice of the kernel on the input. The kernel  $K(x, x') = \text{Id}_{\mathcal{H}_y} k_x(x, x')$  satisfies this assumption. Now we are ready to state the theorem.

**Theorem 3.3.** *[Excess-risk bound, KRR + linear OEL] Let  $\rho$  be a distribution over  $\mathcal{X} \times \mathcal{Y}$ ,  $\rho_y$  the marginal of  $Y$ ,  $(x_i, y_i)_{i=1}^n$  be i.i.d samples from  $\rho$ ,  $(y_i)_{i=1}^m$  i.i.d samples from  $\rho_y$ ,  $\lambda \leq \kappa^2 := \sup_{x \in \mathcal{X}} \|k_x(x, \cdot)\|_{\mathcal{H}_x}$ ,  $\delta > 0$ , and  $M_c$  and  $h_\psi^*$  satisfy Assumption 1 and 2. When*

$$p^r \leq \min \left\{ \frac{\omega m}{9(1-c) \log(m/\delta)}, \frac{\omega n}{9c \log(\frac{n}{\delta})}, \frac{\omega}{8ct_n} \right\}, \quad (14)$$

*then the following holds with probability at least  $1 - 3\delta$ ,*

$$\sqrt{\mathbb{E}_x(\|\tilde{g} \circ \hat{h}_g(x) - h_\psi^*(x)\|^2)} \leq \underbrace{C \frac{Q+R}{\sqrt{\lambda n}} \log^2 \frac{10}{\delta} + R\sqrt{\lambda}}_{\text{KRR excess-risk on linear subspace of dimension } p} + \underbrace{\sqrt{\frac{\Omega'}{p^{(r-1)/2}}}}_{\text{Reconstruction error}},$$

where  $Q = \sup_{y \in \mathcal{Y}} \|k(y, \cdot)\|_{\mathcal{H}_y}$ ,  $R = \|h_\psi^*\|_{\mathcal{H}_x \times \mathcal{H}_y}$ ,  $C = 4\kappa(1 + (4\kappa^2/\sqrt{\lambda n})^{1/2})$ ,  $t_n = \max(Q\sqrt{v_n}, v_n, Qw_n u_n, w_n^2 u_n)$ , with  $u_n = \frac{4\kappa^2 \log \frac{2}{\delta}}{\sqrt{n}}$ ,  $v_n = \mathbb{E}_x(\|\hat{h}_\psi(x) - h_\psi^*\|^2)$ ,  $w_n = (\frac{Q}{\kappa} u_n(1 + \|h_\psi^*\|_{\mathcal{H}}) + \lambda \|h_\psi^*\|_{\mathcal{H}})$ . Finally  $\Omega' = \Omega^{\frac{r+1}{r}} q_r$ ,  $q_r$  a constant depending only on  $r$  (defined in the proof).

The first term in the above bound is the usual bias-variance trade-off that we expect from KRR (c.f. [6]). The second term is an approximation error due to the projection.

We further see a trade-off in the choice of  $c$  when we try to maximize  $p$ . Choosing  $c$  close to one aims to estimate the linear subspace of the  $h^*(x) = \mathbb{E}_{y|x}(\psi(y))$  which is smaller than the one of the  $\psi(y)$  leading to a better eigenvalues decay rate, but the learning is limited by the convergence of the least-square estimator as is clear by the third term of Eq. (14). Choosing  $c$  close to zero leads to completely unsupervised learning of the output embeddings with a smaller eigenvalue decay rate  $r$ .

In the following corollary, we give a simplified version of the bound (we denote by  $a(n) \gtrsim b(n)$  the fact that there exists  $C > 0$  such that  $a(n) \geq Cb(n)$  for  $n \in \mathbb{N}$ ).

**Corollary 3.3.1.** *Under the same assumptions of Theorem 3.3, let  $\lambda = 1/\sqrt{n}$ . Assume  $r \geq 7/2$ . Then, running the proposed algorithm with a number of components*

$$p \gtrsim n^{\frac{1}{r-1}},$$

*is enough to achieve an excess-risk of  $\mathcal{R}(\hat{f}) - \mathcal{R}(f^*) = O(n^{-1/4})$ .*

Note that  $n^{-1/4}$  is the typical rate for problems of structured prediction without further assumptions on the problem [8, 9]. Here it is interesting to note that when the problem is relatively regular, i.e.,  $r \geq 7/2$ , we can achieve such rate with a number of components  $p \ll n$ , in particular  $p = n^{1/(2(r-1))}$ , leading to a relevant improvement in terms of computational complexity.

Finally we note that while from an approximation viewpoint the largest  $p$  would lead to better results, there is still a trade-off with the computational aspects, since an increased  $p$  leads to greater computational complexity. Moreover, we expect to find a more subtle trade-off between the KRR

error and the approximation error due to projection, since reducing the dimensionality of the output space have a beneficial impact on the degrees of freedom of the problem. We observed this effect from an experimental viewpoint and we expect to observe using a more refined analysis, that we leave as future work. We want to conclude with a remark on why projecting on  $M_c$  with  $c \in (0, 1)$  should be more beneficial than just projecting on the subspace spanned by the covariance operator associated to  $\psi(y)$ .

**Remark 3.1** (Supervised learning benefit). *Learning the embedding in a supervised fashion is interesting as the principal components of the  $\psi(y)$  may differ from that of the  $h_\psi^*(x)$ . The most basic example:  $x \in \mathbb{R}$ ,  $\psi(y) \in \mathbb{R}^2$ ,  $x \sim \mathcal{N}(0, \sigma_x^2)$ , with the relationship between  $x$  and  $\psi(y) = (x, z)$  where  $z \sim \mathcal{N}(0, \sigma_z^2)$  independent from  $x$  with  $\sigma_z^2 > \sigma_x^2$ . In this case unsupervised learning is not able to find the 1-dimensional subspace where the  $h_\psi^*(x)$  lie, whereas, supervised learning could do so, assuming  $\hat{h}_\psi$  is a good estimation of  $h_\psi^*$ . From this elementary example we could build more complex and realistic ones, by adding any kind of non-isotropic noise  $z$  that change the shape of the  $h_\psi^*(x)$  subspace. For instance, defining eigenvalue decay of  $h_\psi^*(x)$  and  $z \in \mathcal{H}_y$  with  $z$  lower eigenvalue decay, then for  $p$  sufficiently large the order of principal components start to change (comparing  $h_\psi^*(x)$  and  $\psi(y) := h_\psi^*(x) + z$ ).*

## 4 Experiments

We provide a detailed experimental study of OEL on image reconstruction, multilabel classification and labeled graph prediction. For each dataset/task, we selected the relevant state-of-the-art algorithms to which compare to. Details about experimental protocols (hyperparameter grids, dataset splitting) are provided in the Supplements. Additionally, an exhaustive study on label ranking is also provided in the Supplements. We used the following notations to refer to variants of our method:

$OEL^0$ : ( $\gamma = 0$ ) only reconstruction loss is used to learn  $G$  with data coming only from  $\mathcal{S}_n$   
 $OEL^1$ : ( $\gamma = 1/2$ )  $G$  is learned using both criteria (regression and reconstruction) also using  $\mathcal{S}_n$   
 $OEL^c$  with  $\mathcal{U}_m$ :  $\hat{c} \in [0, 1]$  is selected by inner CV, and additional unlabeled dataset  $\mathcal{U}_m$  is leveraged to learn  $G$ .

**Image reconstruction.** In the image reconstruction problem provided by [40], the goal is to predict the bottom half of a USPS handwritten postal digit (16 x 16 pixels), given its top half. We have  $n = 7291$  labeled images and  $n_{te} = 2007$  test images. Fig. 2 presents the behaviour of OEL in terms of Mean Squared Error of  $G^*G\hat{h}_\psi$  w.r.t.  $\lambda$  and  $p$ , showing that a minimum is attained and highlighting a trade-off between the two regularization parameters. We compared OEL to IOKR [5] and Kernel Dependency Estimation (KDE) [40]. In KDE, KPCA is used to decompose the output feature vectors into  $p$  orthogonal directions. Kernel ridge regression is then used for learning independently the mapping between the input feature vectors and each direction. By applying KPCA on the outputs KDE aims at estimating the linear subspace of the output embedding  $\psi(y)$ , while OEL aims at estimating the linear subspace of the  $h_\psi^*(x)$ . In addition the decoding problem in KDE is different from OEL.

The obtained results are given in Table 1. Firstly, OEL obtains improved results in comparison to IOKR and KDE. Moreover, adding additional unsupervised output data ("+" data) is beneficial. The selected dimensions follow the theoretical insights. Learning the embedding in a supervised fashion ( $OEL^1$  instead of  $OEL^0$ ) allows to learn smaller dimensional embedding giving the same, or even better, performance. Learning the embedding with additional data allows to learn bigger dimensional linear subspace. Furthermore, on this problem, the selected balancing parameter  $c$  is close to  $1/2$ , that is, all output training data are given the same importance.

**Multi-label classification.** Here we compare OEL with several multi-label and structured prediction approaches including IOKR [5], logistic regression (LR) trained independently for each label [23], a two-layer neural network with cross entropy loss (NN) by [2], the multi-label approach PRLR (Posterior-Regularized Low-Rank) [23], the energy-based model SPEN (Structured Prediction Energy Networks) [2] as well as DVN (Deep Value Networks) [14].

The results in Table 2 (left) show that OEL can compete with state-of-the-art dedicated multilabel methods on the standard dataset Bibtex. In a second experiment (Table 2, right) we trained OEL by splitting the datasets in a smaller training set and using the rest of the examples as unsupervised

| Method                                     | RBF loss                            | p        |
|--|-------------------------------------|----------|
| KDE [40]                                   | $0.764 \pm 0.011$                   | 64       |
| IOKR                                       | $0.751 \pm 0.011$                   | $\infty$ |
| OEL <sup>0</sup>                           | $0.737 \pm 0.011$                   | 71       |
| OEL <sup>1</sup>                           | $0.734 \pm 0.011$                   | 64       |
| OEL <sup>c</sup> + data ( $c \in [0, 1]$ ) | <b><math>0.725 \pm 0.011</math></b> | 98       |

Table 1: Test mean losses and standard errors for IOKR, OEL and KDE on the USPS digits reconstruction problem where  $n/m = 1000/6000$ .

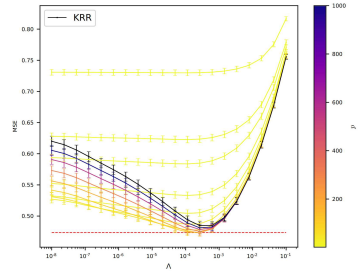


Figure 2: Test MSE w.r.t  $\lambda$  and  $p$  (OEL<sup>c</sup>)

output data. We observe that the OEL obtains higher  $F_1$  scores than IOKR in this setup. Using additional unsupervised data provides further improvement in the case of the Bookmarks and Corel5k datasets.

| Method           | $F_1$                  |                         | Bibtex      | Bookmarks   | Corel5k     |
|------------------|------------------------|-------------------------|-------------|-------------|-------------|
| IOKR             | 44.0 ( $p = +\infty$ ) | $n$                     | 2000        | 2000        | 2000        |
| OEL <sup>1</sup> | 43.8 ( $p = 130$ )     | $m$                     | 2880        | 4000        | 2500        |
| LR [23]          | 37.2                   | $n_{te}$                | 2515        | 2500        | 499         |
| NN [2]           | 38.9                   | IOKR                    | 35.9        | 22.9        | 13.7        |
| SPEN [2]         | 42.2                   | OEL <sup>1</sup>        | <b>39.7</b> | 25.9        | 16.1        |
| PRLR [23]        | 44.2                   | OEL <sup>c</sup> + data | <b>39.7</b> | <b>27.1</b> | <b>19.0</b> |
| DVN [14]         | <b>44.7</b>            |                         |             |             |             |

Table 2: Left:  $F_1$  scores of state-of-the-art methods on Bibtex dataset ( $n/n_{te} = 4880/2515$ ). Right:  $F_1$  score of OEL and IOKR on different multi-label problems in a small training data regime.

**Metabolite Identification.** In metabolite identification, the problem is to predict the molecular structure of a metabolite given its tandem mass spectrum. State-of-the-art results for this problem have been obtained with the IOKR method by [4], where we take the similar numerical experimental protocol (5-CV Outer/4-CV Inner loops) and output kernel (Gaussian-Tanimoto) on the molecular fingerprints. Besides the labeled training set ( $n = 6974$ ), a very large additional dataset of  $10^5$  molecules (candidate outputs), without corresponding inputs (spectra) is available and utilized by OEL. Details can be found in the Supplementary material. Analyzing the results in Table 3, given for three metrics including the top-k-accuracy, we observe that without any additional data, OEL<sup>0</sup> and OEL<sup>1</sup> slightly improved upon plain IOKR and even more when exploiting additional unlabeled data with OEL<sup>c</sup>. Such accuracy improvement is crucial in this real-world task. In OEL<sup>c</sup>, the selected balancing parameter by an inner cross-validation on training set is  $\hat{c} = 0.75$  in average on the outer splits, imposing a balance between the influence of the small size labeled dataset and the large unsupervised output set.

| Method                         | MSE                                 | Tanimoto-Gaussian loss              | Top-k accuracies<br>$k = 1 \mid k = 5 \mid k = 10$ |
|--------------------------------|-------------------------------------|-------------------------------------|--|
| IOKR                           | $0.781 \pm 0.002$                   | $0.463 \pm 0.009$                   | 29.6%   61.1%   71.0%                              |
| OEL <sup>0</sup>               | <b><math>0.765 \pm 0.003</math></b> | $0.463 \pm 0.009$                   | 29.5%   61.1%   70.9%                              |
| OEL <sup>1</sup>               | $0.766 \pm 0.003$                   | $0.459 \pm 0.010$                   | 30.0%   61.5%   71.4%                              |
| OEL <sup>c</sup> + $10^5$ data | <b><math>0.765 \pm 0.003</math></b> | <b><math>0.441 \pm 0.009</math></b> | <b>31.2%   63.5%   72.7%</b>                       |

Table 3: Test mean losses and standard errors for the metabolite identification problem.



## 5 Conclusion

We have presented a novel approach, OEL, for learning output embeddings in structured prediction. The OEL methods allows us to leverage the rich Hilbert space representations of structured outputs while allowing adaptation to particular input spaces and controlling the excess risk of the model through supervised dimensionality reduction in the output space. Our empirical experiments demonstrate the relevance of the method in particular when separate output sample is available. Our experimental results show a state-of-the-art performance or exceeding it for various applications.

## Broader Impact

Making machine learning models that are able to predict structured objects such as molecules have broad applications in society. For example the metabolite identification task has relevance to biomedicine, pharmaceuticals, anti-doping, and regulatory affairs, to name a examples - and structured prediction methods have state-of-the-art performance.

From the theoretical side, understanding how output representations can be learned better is an important consideration both in practice and theory. This paper provides a theoretically well-founded approach, which helps our understanding of how structured prediction methods can be improved.

Potential down-sides of the method are shared with all machine learning: the methods will make errors and human scrutiny may be needed to post-process the predictions before application.

The methods will be provided as open code for the disposal of the society as a whole.

## References

- [1] A. Bakhtin, Y. Deng, S. Gross, M. Ott, M. Ranzato, and A. Szlam. Energy-based models for text. *CoRR*, abs/2004.10188, 2020.
- [2] D. Belanger and A. McCallum. Structured prediction energy networks. In *Proceedings of the 33rd International Conference on International Conference on Machine Learning - Volume 48*, ICML’16, page 983–992. JMLR.org, 2016.
- [3] C. Brouard, F. d’Alché-Buc, and M. Szafranski. Semi-supervised penalized output kernel regression for link prediction. In *Proceedings of the 28th International Conference on Machine Learning*, pages 593–600, 2011.
- [4] C. Brouard, H. Shen, K. Dührkop, F. d’Alché Buc, S. Böcker, and J. Rousu. Fast metabolite identification with input output kernel regression. *Bioinformatics*, 32(12):i28–i36, 2016.
- [5] C. Brouard, M. Szafranski, and F. d’Alché-Buc. Input output kernel regression: Supervised and semi-supervised structured output prediction with operator-valued kernels. *The Journal of Machine Learning Research*, 17(1):6105–6152, 2016.
- [6] A. Caponnetto and E. De Vito. Optimal rates for the regularized least-squares algorithm. *Foundations of Computational Mathematics*, 7(3):331–368, 2007.
- [7] W. Cheng, E. Hüllermeier, and K. J. Dembczynski. Label ranking methods based on the plackett-luce model. In *Proceedings of the 27th International Conference on Machine Learning (ICML-10)*, pages 215–222, 2010.
- [8] C. Ciliberto, L. Rosasco, and A. Rudi. A consistent regularization approach for structured prediction. In *Advances in neural information processing systems*, pages 4412–4420, 2016.
- [9] C. Ciliberto, L. Rosasco, and A. Rudi. A general framework for consistent structured prediction with implicit loss embeddings. *arXiv preprint arXiv:2002.05424*, 2020.
- [10] C. Cortes, M. Mohri, and J. Weston. A general regression technique for learning transductions. In *Proceedings of the 22nd International Conference on Machine Learning*, page 153–160, 2005.
- [11] M. Djerrab, A. Garcia, M. Sangnier, and F. d’Alché Buc. Output fisher embedding regression. *Machine Learning*, 107(8-10):1229–1256, 2018.
- [12] T. Gärtner. *Kernels for Structured Data*, volume 72 of *Series in Machine Perception and Artificial Intelligence*. WorldScientific, 2008.
- [13] P. Geurts, L. Wehenkel, and F. d’Alché Buc. Kernelizing the output of tree-based methods. In *Proceedings of the 23rd international conference on Machine learning*, pages 345–352, 2006.
- [14] M. Gygli, M. Norouzi, and A. Angelova. Deep value networks learn to evaluate and iteratively refine structured outputs. In *Proceedings of the 34th International Conference on Machine Learning - Volume 70*, ICML’17, page 1341–1351, 2017.

- [15] N. Halko, P.-G. Martinsson, and J. A. Tropp. Finding structure with randomness: Probabilistic algorithms for constructing approximate matrix decompositions. *SIAM review*, 53(2):217–288, 2011.
- [16] E. Hüllermeier, J. Fürnkranz, W. Cheng, and K. Brinker. Label ranking by learning pairwise preferences. *Artificial Intelligence*, 172(16):1897 – 1916, 2008.
- [17] H. Kadri, M. Ghavamzadeh, and P. Preux. A generalized kernel approach to structured output learning. In *International Conference on Machine Learning*, pages 471–479, 2013.
- [18] I. Katakis, G. Tsoumakas, and I. Vlahavas. Multilabel text classification for automated tag suggestion. *ECML PKDD Discovery Challenge 2008*, page 75, 2008.
- [19] A. Korba, A. Garcia, and F. d’Alché Buc. A structured prediction approach for label ranking. In *Advances in Neural Information Processing Systems*, pages 8994–9004, 2018.
- [20] P. Laforgue, S. Cléménçon, and F. d’Alché Buc. Autoencoding any data through kernel autoencoders. In *The 22nd International Conference on Artificial Intelligence and Statistics*, pages 1061–1069, 2019.
- [21] P. Laforgue, A. Lambert, L. Motte, and F. d’Alché Buc. On the dualization of operator-valued kernel machines. *arXiv preprint arXiv:1910.04621*, 2019.
- [22] M. Lapin, M. Hein, and B. Schiele. Loss functions for top-k error: Analysis and insights. In *2016 IEEE Conference on Computer Vision and Pattern Recognition, CVPR 2016, Las Vegas, NV, USA, June 27-30, 2016*, pages 1468–1477. IEEE Computer Society, 2016. doi: 10.1109/CVPR.2016.163. URL <https://doi.org/10.1109/CVPR.2016.163>.
- [23] X. V. Lin, S. Singh, L. He, B. Taskar, and L. Zettlemoyer. Multi-label learning with posterior regularization. In *NIPS Workshop on Modern Machine Learning and Natural Language Processing*, 2014.
- [24] G. Luise, D. Stamos, M. Pontil, and C. Ciliberto. Leveraging low-rank relations between surrogate tasks in structured prediction. In *International Conference on Machine Learning*, pages 4193–4202, 2019.
- [25] M. Mohri, A. Rostamizadeh, and A. Talwalkar. *Foundations of Machine Learning*. The MIT Press, 2012. ISBN 026201825X, 9780262018258.
- [26] D. H. Nguyen, C. H. Nguyen, and H. Mamitsuka. Recent advances and prospects of computational methods for metabolite identification: a review with emphasis on machine learning approaches. *Briefings in bioinformatics*, 20(6):2028–2043, 2019.
- [27] A. Nowak-Vila, F. Bach, and A. Rudi. A general theory for structured prediction with smooth convex surrogates. *arXiv preprint arXiv:1902.01958*, 2019.
- [28] S. Nowozin and C. H. Lampert. Structured learning and prediction in computer vision. *Found. Trends Comput. Graph. Vis.*, 6(3-4):185–365, 2011.
- [29] A. Osokin, F. R. Bach, and S. Lacoste-Julien. On structured prediction theory with calibrated convex surrogate losses. In *Advances in Neural Information Processing Systems 30*, pages 302–313, 2017.
- [30] M. Palatucci, D. Pomerleau, G. E. Hinton, and T. M. Mitchell. Zero-shot learning with semantic output codes. In *Advances in neural information processing systems*, pages 1410–1418, 2009.
- [31] V. K. Pillutla, V. Roulet, S. M. Kakade, and Z. Harchaoui. A smoother way to train structured prediction models. In *Advances in Neural Information Processing Systems*, pages 4766–4778, 2018.
- [32] A. Rudi, G. D. Cañas, and L. Rosasco. On the sample complexity of subspace learning. In *Advances in Neural Information Processing Systems*, pages 2067–2075, 2013.

- [33] A. Rudi, L. Carratino, and L. Rosasco. Falcon: An optimal large scale kernel method. In *Advances in Neural Information Processing Systems*, pages 3888–3898, 2017.
- [34] B. Schölkopf, A. J. Smola, and K. Müller. Nonlinear component analysis as a kernel eigenvalue problem. *Neural Computation*, 10(5):1299–1319, 1998.
- [35] K. Sohn, H. Lee, and X. Yan. Learning structured output representation using deep conditional generative models. In *Advances in neural information processing systems*, pages 3483–3491, 2015.
- [36] K. Struminsky, S. Lacoste-Julien, and A. Osokin. Quantifying learning guarantees for convex but inconsistent surrogates. In *Advances in Neural Information Processing Systems*, pages 669–677, 2018.
- [37] B. Taskar, C. Guestrin, and D. Koller. Max-margin markov networks. In *Advances in neural information processing systems*, pages 25–32, 2004.
- [38] I. Tsochantaridis, T. Hofmann, T. Joachims, and Y. Altun. Support vector machine learning for interdependent and structured output spaces. In *Proceedings of the twenty-first international conference on Machine learning*, page 104, 2004.
- [39] G. Tsoumakas and I. Katakis. Multi-label classification: An overview. *IJDWM*, 3(3):1–13, 2007.
- [40] J. Weston, O. Chapelle, V. Vapnik, A. Elisseeff, and B. Schölkopf. Kernel dependency estimation. In *Advances in neural information processing systems*, pages 897–904, 2003.

## 6 Supplementary material

### 6.1 Definitions and Notation

Here we introduce, and give basic properties, on the ideal and empirical linear operators that we will use in the following to prove the excess-risk theorem.

- $\phi : \mathcal{X} \rightarrow \mathcal{H}_x, \forall x \in \mathcal{X}, \phi(x) = k_x(x, \cdot)$
- $S : f \in \mathcal{H}_x \rightarrow \langle f, k_x(x, \cdot) \rangle_{\mathcal{H}_x} \in L^2(\mathcal{X}, \rho_{\mathcal{X}})$
- $Z : h \in \mathcal{H}_y \rightarrow \langle h, h^*(\cdot) \rangle_{\mathcal{H}_y} \in L^2(\mathcal{X}, \rho_{\mathcal{X}})$ , (with  $h^*(x) := \mathbb{E}_{y|x}(\psi(y))$ )
- $S_n : f \in \mathcal{H}_x \rightarrow \frac{1}{\sqrt{n}}(\langle f, k_x(x_i, \cdot) \rangle_{\mathcal{H}_x})_{1 \leq i \leq n} \in \mathbb{R}^n$
- $Z_n : h \in \mathcal{H}_y \rightarrow \frac{1}{\sqrt{n}}(\langle h, \psi(y_i) \rangle_{\mathcal{H}_y})_{1 \leq i \leq n} \in \mathbb{R}^n$
- $C = \mathbb{E}_x(\phi(x) \otimes \phi(x)) = S^*S$  and its empirical counterpart  $C_n = \frac{1}{n} \sum_{i=1}^n \phi(x_i) \otimes \phi(x_i)$
- $V = \mathbb{E}_y(\psi(y) \otimes \psi(y))$  and its empirical counterpart  $V_n = \frac{1}{m} \sum_{i=1}^m \psi(y_i) \otimes \psi(y_i)$
- $N = \mathbb{E}_x(h^*(x) \otimes h^*(x)) = HCH^*$  (with  $H = Z^*SC^\dagger$ ) and its empirical counterpart  $N_n = H_nC_nH_n^*$  (with  $H_n = Z_n^*S_n(C_n + \lambda I)^{-1}$ ).
- $M_c = cN + (1 - c)V$  and its empirical counterpart  $\hat{M}_c = cN_n + (1 - c)V_m$
- $h_\psi^*(\cdot) = H\phi(\cdot)$  and its empirical counterpart  $\hat{h}_\psi(\cdot) = H_n\phi(\cdot)$
- The gamma function  $\Gamma : z \rightarrow \int_0^\infty t^{z-1}e^{-t}dt$

We have the following properties:

- $Z^*S = \int_{\mathcal{X} \times \mathcal{Y}} \psi(y) \otimes \phi(x) d\rho(x, y)$
- $Z_n^*S_n = \frac{1}{n} \sum_{i=1}^n \psi(y_i) \otimes \phi(x_i)$
- If  $h^*(x) := \mathbb{E}_{y|x}(\psi(y)) \in \mathcal{H}$ , then  $h^*(x) = H\phi(x)$ ,  $\forall x \in \mathcal{X}$ , with  $H = Z^*SC^\dagger \in \mathcal{H}_y \otimes \mathcal{H}_x$
- $\forall \lambda > 0, \hat{h}(x) = H_n\phi(x)$ ,  $\forall x \in \mathcal{X}$ , with  $H_n = Z_n^*S_n(C_n + \lambda I)^{-1} \in \mathcal{H}_y \otimes \mathcal{H}_x$

### 6.2 Lemmas

First, we give the following lemma showing the equivalence in the linear case between the general initial objective (3) and the mixed linear subspace estimation one (6).

**Lemma 6.1.** *Using the solution of the  $\psi(Y)$  regression problem, Eq. (5) is equivalent to:*

$$\min_G \gamma \mathbb{E}_X[\|G^*Gh_\psi^*(X) - h_\psi^*(X)\|_{\mathcal{H}_y}^2] + (1 - 2\gamma) \mathbb{E}_Y[\|G^*G\psi(Y) - \psi(Y)\|_{\mathcal{H}_y}^2]. \quad (15)$$

*Proof.* In the linear case, (3) instantiates as

$$\min_G \gamma \mathbb{E}_{X,Y}[\|G(h_\psi^*(X) - \psi(Y))\|_{\mathbb{R}^p}^2] + (1 - \gamma) \mathbb{E}_Y[\|G^*G\psi(Y) - \psi(Y)\|_{\mathcal{H}_y}^2]. \quad (16)$$

Decomposing the first term, with  $h_\psi^*(x) = \mathbb{E}_{Y|X=x}[\psi(Y)]$ , and noticing that  $\|G\psi(y)\|_{\mathbb{R}^p} = \|G^*G\psi(y)\|_{\mathcal{H}_y}$  ( $G$  is orthogonal), one can check that we obtain the desired result.  $\square$

From here, we give the lemmas, and their proofs, that we used in order to prove the main theorem in the next section.

First, we leverage the *comparison inequality* from [8], allowing to relate the excess-risk of  $f = d \circ \tilde{g} \circ h$  to the  $L^2$  distance of  $\tilde{g} \circ \hat{h}$  to  $h_\psi^*$ .

**Lemma 3.1.** For every measurable  $\hat{h} : \mathcal{X} \rightarrow \mathbb{R}^p, \tilde{g} : \mathbb{R}^p \rightarrow \mathcal{H}_y, f = d \circ \tilde{g} \circ \hat{h}$ ,

$$\mathcal{R}(f) - \mathcal{R}(f^*) \leq c(\psi) \sqrt{\mathbb{E}_X \|\tilde{g} \circ \hat{h}(X) - h_\psi^*(X)\|_{\mathcal{H}_y}^2}$$

with  $c(\psi) = 2\sqrt{2Q^2 + Q^4 + 1}$ ,  $Q = \sup_{y \in \mathcal{Y}} \|\psi(y)\|^2$ .

*Proof.* The considered loss function  $\Delta(y, y') = \|\psi(y) - \psi(y')\|_{\mathcal{H}_y}^2$  belongs to the wide family of SELF losses [8] for which the comparison inequality holds. A loss is SELF if it satisfies the *implicit embedding property* [9], i.e. there exists an Hilbert space  $\mathcal{V}$  and two feature maps  $\gamma, \theta : \mathcal{Y} \rightarrow \mathcal{V}$  such that

$$\Delta(y, y') = \langle \gamma(y), \theta(y') \rangle_{\mathcal{V}}, \quad \forall y, y' \in \mathcal{Y}.$$

In our case the construction is direct and corresponds to  $\mathcal{V} = \mathcal{H}_y \oplus \mathbb{R} \oplus \mathbb{R}$ ,  $\gamma(y) = (\sqrt{2}\psi(y), \|\psi(y)\|_{\mathcal{H}_y}^2, 1)$  and  $\theta(y') = (-\sqrt{2}\psi(y'), 1, \|\psi(y')\|_{\mathcal{H}_y}^2)$

Hence, directly applying Theorem 3. from [9], we get a constant:

$$c_\Delta = 2 \times \sup_{y \in \mathcal{Y}} \|\gamma(y)\| = 2 \sup_{y \in \mathcal{Y}} \sqrt{2\|\psi(y)\|^2 + \|\psi(y)\|^4 + 1} = 2\sqrt{2Q^2 + Q^4 + 1}$$

□

In the theorem's proof, we will split the surrogate excess-risk of  $\tilde{g} \circ \hat{h}$ , using triangle inequality, in two terms: 1) the KRR excess-risk of  $\hat{h}$  in estimating the new embedding  $g$ , 2) the excess-risk or reconstruction error of the learned couple  $(g, \tilde{g})$  when recovering  $\psi$ . For now,  $g, \tilde{g}$  are supposed to be of the form:  $g : y \rightarrow G\psi(y), \tilde{g} : z \rightarrow G^*z$ , with  $G \in \mathbb{R}^p \otimes \mathcal{H}_y$  such that  $GG^* = I_{\mathbb{R}^p}$ .

The following lemma give a bound for the first term: the KRR excess-risk on the learned linear subspace of dimension  $p$ . To do so, we simply bound it with the KRR excess-risk on the entire space  $\mathcal{H}_y$ , and leave as a future work a refined analysis of this term studying its dependency w.r.t  $p$ .

**Lemma 6.2** (Kernel Ridge Excess-risk Bound on a linear subspace of dimension  $p$ ). *Let be  $\hat{G} \in \mathbb{R}^p \otimes \mathcal{H}_y$  such that  $\hat{G}\hat{G}^* = I_{\mathbb{R}^p}$ , then with probability at least  $1 - \delta$ :*

$$\sqrt{\mathbb{E}_x(\|\hat{G}^*\hat{G}(\hat{h}_\psi(x) - h_\psi^*(x))\|^2)} \leq C \frac{Q + R}{\sqrt{\lambda n}} \log^2 \frac{10}{\delta} + R\sqrt{\lambda}$$

with  $Q := \sup_{y \in \mathcal{Y}} \|\psi(y)\|_{\mathcal{H}_y}$ ,  $R = \|h_\psi^*\|_{\mathcal{H}_x \times \mathcal{H}_y}$ ,  $C = 4\kappa(1 + (4\kappa^2/\sqrt{\lambda n})^{1/2})$ .

*Proof.* We observe that:  $\sqrt{\mathbb{E}_x(\|\hat{G}^*\hat{G}(\hat{h}_\psi(x) - h_\psi^*(x))\|^2)} \leq \sqrt{\mathbb{E}_x(\|\hat{h}_\psi(x) - h_\psi^*(x)\|_{\mathcal{H}_y}^2)}$

Then, considering the assumptions of Theorem 3.3, we use result for kernel ridge regression from [8], with  $Q := \sup_{y \in \mathcal{Y}} \|\psi(y)\|_{\mathcal{H}_y}$ ,  $R = \|h_\psi^*\|_{\mathcal{H}_x \times \mathcal{H}_y}$ ,  $C = 4\kappa(1 + (4\kappa^2/\sqrt{\lambda n})^{1/2})$ .

□

Then, we show that we can upper bound the reconstruction error term, using Jensen inequality, by the ideal counterpart of the empirical objective w.r.t the output embedding  $G$  of the algorithm 1.

**Lemma 3.2.** *Under the assumptions of Lemma 3.1, when  $\tilde{g}$  is a linear projection, we have*

$$\mathbb{E}_x[\|\tilde{g}(h_g^*(x)) - h_\psi^*(x)\|^2] \leq \langle I - P, M_c \rangle_{\mathcal{H}_y \otimes \mathcal{H}_y}$$

*Proof.* Let  $c \in [0, 1]$ ,  $G \in \mathbb{R}^p \otimes \mathcal{H}_y$  such that  $GG^* = I_{\mathbb{R}^p}$ ,  $g : y \rightarrow G\psi(y), \tilde{g} : z \rightarrow G^*z$

Defining the projection  $P = G^*G \in \mathcal{H}_y \times \mathcal{H}_y$ , we have

$$\begin{aligned}
\mathbb{E}_x[\|\tilde{g}(h_g^*(x)) - h_\psi^*(x)\|^2] &= \mathbb{E}_x(\|Ph_\psi^*(x) - h_\psi^*(x)\|^2) \\
&= c\mathbb{E}_x(\|Ph_\psi^*(x) - h_\psi^*(x)\|^2) + (1-c)\mathbb{E}_x(\|Ph_\psi^*(x) - h_\psi^*(x)\|^2) \\
&= c\mathbb{E}_x(\|Ph_\psi^*(x) - h_\psi^*(x)\|^2) + (1-c)\mathbb{E}_x(\|P\mathbb{E}_{y|x}(\psi(y)) - \mathbb{E}_{y|x}(\psi(y))\|^2) \\
&\leq c\mathbb{E}_x(\|Ph^*(x) - h^*(x)\|^2) + (1-c)\mathbb{E}_y(\|P\psi(y) - \psi(y)\|^2) \quad (\text{Jensen's inequality}) \\
&= c\langle I - P, \mathbb{E}_x(h^*(x) \otimes h^*(x)) \rangle_{\mathcal{H}_y \otimes \mathcal{H}_y} + (1-c)\langle I - P, \mathbb{E}_y(\psi(y) \otimes \psi(y)) \rangle_{\mathcal{H}_y \otimes \mathcal{H}_y} \\
&= \langle I - P, M_c \rangle_{\mathcal{H}_y \otimes \mathcal{H}_y}
\end{aligned}$$

□

Then, the following lemma study the efficiency of our algorithm in minimizing  $\langle I - \hat{G}^*\hat{G}, M_c \rangle_{\mathcal{H}_y \otimes \mathcal{H}_y}$ . To do so, we followed the approach of [32], with the help of an additional necessary technical lemma 6.4.

**Lemma 6.3** (OEL Subspace estimation). *If  $t_{min} \leq t \leq \min(\|V\|_\infty, \|N\|_\infty)$ , with probability  $1 - 3\delta$ :*

$$\sqrt{\langle I - \hat{G}^*\hat{G}, M_c \rangle_{\mathcal{H}_y \otimes \mathcal{H}_y}} \leq 3\Omega't^{-1/2r} \sqrt{\sigma_k(M_c) + t}$$

with:  $t_{min} = \max((1-c)t_1, ct_2)$ , and  $t_1 = \frac{9}{m} \log(\frac{m}{\delta})$ ,  $t_2 = 5 \max(4c^2v_n, 2cv_n, 4cRw_nu_n, 2cw_n^2u_n, 2R^2u_n)$ , with  $u_n = \frac{4\kappa^2 \log \frac{2}{\delta}}{\sqrt{n}}$ ,  $v_n = \mathbb{E}_x(\|\hat{h}_\psi(x) - h_\psi^*\|^2)$ ,  $w_n = (\frac{Q}{\lambda\kappa}u_n(1+R) + \lambda R)$ , and  $\Omega' = (\Omega^{1/r}\Gamma(1-1/r)\Gamma(1+1/r)\Gamma(1/r))^{1/2}$ ,  $R = \|h_\psi^*\|_{\mathcal{H}}$ .

*Proof.* Let be  $c \in [0, 1]$ , we have from Proposition C.4. in [32]:

$$\langle I - \hat{G}^*\hat{G}, M_c \rangle_{\mathcal{H}_y \otimes \mathcal{H}_y} = \|(\hat{G}^*\hat{G} - I)M_c^{\frac{1}{2}}\|_{HS}^2 \quad (17)$$

Then, following [32] proofs, we split (17) into three parts, and bound each term,

$$\|(\hat{G}^*\hat{G} - I)M_c^{\frac{1}{2}}\|_{HS} \leq \underbrace{\|(M_c + tI)^{\frac{1}{2}}(\hat{M}_c + tI)^{-\frac{1}{2}}\|_\infty}_{\mathcal{A}} \times \underbrace{(\sigma_k(\hat{M}_c) + t)^{\frac{1}{2}}}_{\mathcal{B}} \times \underbrace{\|(M_c + tI)^{-\frac{1}{2}}M_c^{\frac{1}{2}}\|_{HS}}_{\mathcal{C}}$$

**[Bound  $\mathcal{A} = \|(M_c + tI)^{\frac{1}{2}}(\hat{M}_c + tI)^{-\frac{1}{2}}\|_\infty]$**  We apply Lemma 6.4, which gives if  $t_{min} \leq t \leq \min(\|V\|_\infty, \|N\|_\infty)$ . Then with probability  $1 - 3\delta$  it is

$$\frac{2}{3} \leq \|(M_c + tI)^{\frac{1}{2}}(\hat{M}_c + tI)^{-\frac{1}{2}}\|_\infty \leq 2$$

**[Bound  $\mathcal{B} = (\sigma_k(\hat{M}_c) + t)^{\frac{1}{2}}$ ]** As in Lemma 3.5 in [32] (cf. Lemma B.2 point 4), the previous lower bound  $\frac{2}{3}\sqrt{\frac{2}{3}} \leq \|(M_c + tI)^{\frac{1}{2}}(\hat{M}_c + tI)^{-\frac{1}{2}}\|_\infty$  gives us that:

$$\sqrt{\sigma_k(\hat{M}_c) + t} \leq \frac{3}{2}\sqrt{\sigma_k(M_c) + t}$$

**[Bound  $\mathcal{C} = \|(M_c + tI)^{-\frac{1}{2}}M_c^{\frac{1}{2}}\|_{HS}$ ]** Lemma 3.7 of [32] with the eigenvalue decay assumption of our theorem gives us that:

$$\|(M_c + tI)^{-\frac{1}{2}}M_c^{\frac{1}{2}}\|_{HS} \leq \Omega't^{-\frac{1}{2r}}$$

with:  $\Omega' = (\Omega^{1/r}\Gamma(1-1/r)\Gamma(1+1/r)\Gamma(1/r))^{1/2}$

Finally, we get the wanted upper bound on  $\sqrt{\langle I - \hat{G}^*\hat{G}, M_c \rangle_{\mathcal{H}_y \otimes \mathcal{H}_y}}$ .

□

The following lemma is the technical lemma necessary in lemma 6.3's proof to bound the 2 first terms ( $\mathcal{A}$  and  $\mathcal{B}$ ) in the decomposition of the reconstruction error.

**Lemma 6.4** (Term  $\mathcal{A}$ ). *Let  $t_{\min} \leq t \leq \min(\|V\|_\infty, \|N\|_\infty)$ . Then with probability  $1 - 3\delta$  it is*

$$\frac{2}{3} \leq \|(M_c + tI)^{\frac{1}{2}}(\hat{M}_c + tI)^{-\frac{1}{2}}\|_\infty \leq 2$$

with:  $t_{\min} = \max((1 - c)t_1, ct_2)$ , and  $t_1 = \frac{9}{m} \log(\frac{m}{\delta})$ ,  $t_2 = 5 \max(4c^2v_n, 2cv_n, 4cRw_nu_n, 2cw_n^2u_n, 2R^2u_n)$ , with  $u_n = \frac{4\kappa^2 \log \frac{2}{\delta}}{\sqrt{n}}$ ,  $v_n = \mathbb{E}_x(\|\hat{h}_\psi(x) - h_\psi^*\|^2)$ ,  $w_n = (\frac{Q}{\lambda\kappa}u_n(1 + R) + \lambda R)$ ,  $R = \|h_\psi^*\|_{\mathcal{H}}$ .

*Proof.* We will decompose this term to study separately the convergence of  $V_m$  to  $V$ , and the convergence of  $N_n = H_n C_n H_n^*$  to  $N = HCH^*$ . However, in order to study the convergence of  $N_n$  to  $N$  we will need to do an additional decomposition as  $N$  is estimated thanks to the KRR estimation  $H_n$  of  $H$ . So, we do the two decompositions leading to the two terms (1), (2), and then we bound each term:

$$\begin{aligned} \|(M_c + tI)^{\frac{1}{2}}(\hat{M}_c + tI)^{-\frac{1}{2}}\|_\infty &= \|(cN + (1 - c)V + tI)^{\frac{1}{2}}(cN_n + (1 - c)V_m + tI)^{-\frac{1}{2}}\|_\infty \\ &\leq \underbrace{\|(cN + (1 - c)V + tI)^{\frac{1}{2}}(cN + (1 - c)V_m + tI)^{-\frac{1}{2}}\|_\infty}_{(1)} \\ &\quad \times \underbrace{\|(cN + (1 - c)V_m + tI)^{\frac{1}{2}}(cN_n + (1 - c)V_m + tI)^{-\frac{1}{2}}\|_\infty}_{(2)} \end{aligned}$$

**[Bound (1)]** We apply lemma 6.5 and get, if  $\frac{9}{m} \log(\frac{m}{\delta}) \leq t \leq \|V\|_\infty$ , with probability  $1 - \delta$ :  $\sqrt{\frac{2}{3}} \leq (1) \leq \sqrt{2}$

**[Bound (2)]** We write:  $\|(cHCH^* + (1 - c)V_m + tI)^{\frac{1}{2}}(cH_n C_n H_n^* + (1 - c)V_m + tI)^{-\frac{1}{2}}\|_\infty = \|(I - B_n)^{-1}\|_\infty^{1/2}$

with:  $B_n = (cHCH^* + (1 - c)V_m + tI)^{-\frac{1}{2}}c(H_n C_n H_n^* - HCH^*)(cHCH^* + (1 - c)V_m + tI)^{-\frac{1}{2}}$  and:

$$\|B_n\|_\infty \leq \|(cHCH^* + tI)^{-\frac{1}{2}}c(H_n C_n H_n^* - HCH^*)(cHCH^* + tI)^{-\frac{1}{2}}\|_\infty$$

We apply lemma 6.7, and if  $t \geq 5 \max(4c^2v_n, 2cv_n, 4cRw_nu_n, 2cw_n^2u_n, 2R^2u_n)$  with probability  $1 - 2\delta$ ,  $\sqrt{\frac{2}{3}} \leq (2) \leq \sqrt{2}$

**[Conclusion]** As  $(\mathcal{A}) = (1) \times (2)$ , we conclude by union bound with probability  $1 - 3\delta$ , the bound on  $\mathcal{A}$ :  $\frac{2}{3} \leq \mathcal{A} \leq 2$

□

The next three lemmas are technical lemmas about convergences used in the proof of lemma 6.4.

**Lemma 6.5** (Convergence of covariance operator). *Let be  $H \in \mathcal{H}_y \otimes \mathcal{H}_x$ ,  $A = \mathbb{E}_x[H\phi(x) \otimes H\phi(x)]$ ,  $A_n = \frac{1}{n} \sum_{i=1}^n H\phi(x_i) \otimes H\phi(x_i)$ ,  $B \in \mathcal{H}_y \otimes \mathcal{H}_y$  positive semi-definite,  $\frac{9}{n} \log(\frac{n}{\delta}) \leq t \leq \|A\|_\infty$ , with probability  $1 - \delta$  it is*

$$\sqrt{\frac{2}{3}} \leq \|(A + B + tI)^{\frac{1}{2}}(A_n + B + tI)^{-\frac{1}{2}}\|_\infty \leq \sqrt{2}$$

*Proof.* We write:

$$\|(A + B + tI)^{\frac{1}{2}}(A_n + B + tI)^{-\frac{1}{2}}\|_\infty = \|(I - B_n)^{-1}\|_\infty^{1/2}$$



with:  $B_n = (A + B + tI)^{-\frac{1}{2}}(A_n - A)(A + B + tI)^{-\frac{1}{2}}$  and:

$$\begin{aligned}\|B_n\|_\infty &= \|(A + B + tI)^{-\frac{1}{2}}(A_n - A)(A + B + tI)^{-\frac{1}{2}}\|_\infty \\ &\leq \|(A + tI)^{-\frac{1}{2}}(A_n - A)(cM + tI)^{-\frac{1}{2}}\|_\infty\end{aligned}$$

We apply Lemma 3.6 of [32] and get with probability  $1 - \delta$ , if  $\frac{9}{n} \log(\frac{n}{\delta}) \leq t \leq \|A\|_\infty$

$$\|(A + tI)^{-\frac{1}{2}}(A_n - A)(A + tI)^{-\frac{1}{2}}\|_\infty \leq \frac{1}{2}$$

and we conclude as in Lemma 3.6 of [32]. □

**Lemma 6.6** (Bound  $\|H_n - H\|_\infty$ ). *Let be  $u_n = \frac{4\kappa^2 \log \frac{2}{\delta}}{\sqrt{n}}$ , with probability  $1 - 2\delta$  it is*

$$\|H_n - H\|_\infty \leq \frac{Q}{\kappa\lambda} u_n (1 + \|h_\psi^*\|_{\mathcal{H}}) + \lambda \|h_\psi^*\|_{\mathcal{H}}$$

*Proof.* In order to bound  $\|H_n - H\|_\infty$  we do the following decomposition in three terms, and bound each term:

$$\begin{aligned}\|H_n - H\|_\infty &= \|Z_n^* S_n (C_n + \lambda I)^{-1} - Z^* S C^\dagger\|_\infty \\ &\leq \underbrace{\|(Z_n^* S_n - Z^* S)(C_n + \lambda I)^{-1}\|_\infty}_{(A)} + \underbrace{\|Z^* S((C_n + \lambda I)^{-1} - (C + \lambda I)^{-1})\|_\infty}_{(B)} \\ &\quad + \underbrace{\|Z^* S((C + \lambda I)^{-1} - C^\dagger)\|_\infty}_{(C)}\end{aligned}$$

**[Bound (A)]** We have:

$$(A) = \|(Z_n^* S_n - Z^* S)(C_n + \lambda I)^{-1}\|_\infty \leq \frac{1}{\lambda} \|Z_n^* S_n - Z^* S\|_{HS}$$

From [8] (proof of lemma 18.), with probability  $1 - \delta$ :  $(A) \leq \frac{4Q\kappa \log \frac{2}{\delta}}{\lambda\sqrt{n}}$ .

**[Bound (B)]** We have:

$$\begin{aligned}(B) &= \|Z^* S((C + \lambda I)^{-1} - (C_n + \lambda I)^{-1})\|_\infty \\ &= \|Z^* S((C + \lambda I)^{-1}(C_n - C)(C_n + \lambda I)^{-1})\|_\infty \\ &\leq \|Z^* S(C + \lambda I)^{-1}\|_\infty \|C_n - C\|_\infty \|(C_n + \lambda I)^{-1}\|_\infty \\ &\leq \frac{1}{\lambda} \|h_\psi^*\|_{\mathcal{H}} \|C_n - C\|_\infty\end{aligned}$$

where we used the fact that for two invertible operators  $A, B$ :  $A^{-1} - B^{-1} = A^{-1}(B - A)B^{-1}$ , and noting that  $\|Z^* S(C + \lambda I)^{-1}\|_\infty \leq \|Z^* S(C + \lambda I)^{-1}\|_{HS} \leq \|H\|_{HS} = \|h_\psi^*\|_{\mathcal{H}}$ . From [8], with probability  $1 - \delta$ :  $(B) \leq \frac{4\|h_\psi^*\|_{\mathcal{H}} Q\kappa \log \frac{2}{\delta}}{\lambda\sqrt{n}}$ .

**[Bound (C)]** We have:

$$\begin{aligned}(C) &= \|Z^* S((C + \lambda I)^{-1} - C^\dagger)\|_\infty \\ &= \lambda \|Z^* S(C + \lambda I)^{-1}\|_\infty \\ &\leq \lambda \|h_\psi^*\|_{\mathcal{H}}\end{aligned}$$

We conclude now by union bound, with probability at least  $1 - 2\delta$ :

$$\|H_n - H\|_\infty \leq \frac{4Q\kappa \log \frac{2}{\delta}}{\lambda\sqrt{n}} + \frac{4\|h_\psi^*\|_{\mathcal{H}} Q\kappa \log \frac{2}{\delta}}{\lambda\sqrt{n}} + \lambda \|h_\psi^*\|_{\mathcal{H}}$$

□

**Lemma 6.7.** If  $B_n = (cHCH^* + tI)^{-\frac{1}{2}}c(H_nC_nH_n^* - HCH^*)(cHCH^* + tI)^{-\frac{1}{2}}$ , and  $t \geq 5 \max(4c^2v_n, 2cv_n, 4cRw_nu_n, 2cu_n^2, 2R^2u_n)$ , with probability  $1 - 2\delta$  it is

$$\|B_n\|_\infty \leq \frac{1}{2}$$

with  $u_n = \frac{4\kappa^2 \log \frac{2}{\delta}}{\sqrt{n}}$ ,  $v_n = \mathbb{E}_x(\|\hat{h}_\psi(x) - h_\psi^*\|^2)$ ,  $w_n = (\frac{Q}{\lambda\kappa}u_n(1+R) + \lambda R)$ ,  $R = \|h_\psi^*\|_{\mathcal{H}}$

*Proof.* Here, we do the following decomposition in 7 terms in order to only have a sum of product of empirical estimators appearing only in term of difference with their ideal target. Then we will bound each associated term in  $\|B_n\|_\infty = \|(cHCH^* + tI)^{-\frac{1}{2}}c(H_nC_nH_n^* - HCH^*)(cHCH^* + tI)^{-\frac{1}{2}}\|_\infty$ .

$$\begin{aligned} H_nC_nH_n^* - HCH^* &= (H_n - H)CH^* \quad (i) \\ &\quad + HC(H_n - H)^* \quad (ii) \\ &\quad + (H_n - H)C(H_n - H)^* \quad (iii) \\ &\quad + (H_n - H)(C_n - C)H^* \quad (iv) \\ &\quad + H(C_n - C)(H_n - H)^* \quad (v) \\ &\quad + (H_n - H)(C_n - C)(H_n - H)^* \quad (vi) \\ &\quad + H(C_n - C)H^* \quad (vii) \end{aligned}$$

**[Bound (i) and (ii)]**

$$\begin{aligned} \|(cHCH^* + tI)^{-\frac{1}{2}}cHC(H_n - H)^*(cHCH^* + tI)^{-\frac{1}{2}}\|_\infty &\leq c\|(cHCH^* + tI)^{-\frac{1}{2}}HS^*\|_\infty \\ &\quad \times \|(cHCH^* + tI)^{-\frac{1}{2}}(H_n - H)S^*\|_\infty \end{aligned}$$

But:

$$\begin{aligned} \|(cHCH^* + tI)^{-\frac{1}{2}}HS^*\|_\infty &= \|(cHCH^* + tI)^{-\frac{1}{2}}HS^*SH^*(cHCH^* + tI)^{-\frac{1}{2}}\|_\infty^2 \\ &= \|(cHCH^* + tI)^{-\frac{1}{2}}HCH^*(cHCH^* + tI)^{-\frac{1}{2}}\|_\infty^2 \\ &\leq 1 \end{aligned}$$

And:

$$\begin{aligned} \|(cHCH^* + tI)^{-\frac{1}{2}}(H_n - H)S^*\|_\infty &\leq \frac{1}{\sqrt{t}}\|(H_n - H)S^*\|_\infty \\ &= \frac{1}{\sqrt{t}}\sqrt{\mathbb{E}_x(\|\hat{h}(x) - h^*(x)\|^2)} \end{aligned}$$

**[Bound (iii)]**

$$\|(cHCH^* + tI)^{-\frac{1}{2}}(H_n - H)C(H_n - H)^*(cHCH^* + tI)^{-\frac{1}{2}}\|_\infty \leq \frac{c}{t}\mathbb{E}_x(\|\hat{h}(x) - h^*(x)\|^2)$$

**[Bound (iv) and (v)]**

$$\begin{aligned} \|(cHCH^* + tI)^{-\frac{1}{2}}(H_n - H)(C_n - C)H^*(cHCH^* + tI)^{-\frac{1}{2}}\|_\infty &\leq \frac{c}{t}\|H_n - H\|_\infty\|C_n - C\|_\infty\|H\|_\infty \\ &\leq \frac{c}{t}R\|H_n - H\|_\infty\|C_n - C\|_\infty, \end{aligned}$$

noting  $R = \|h_\psi^*\|_{\mathcal{H}}$ .

**[Bound (vi)]**

$$\|(cHCH^* + tI)^{-\frac{1}{2}}(H_n - H)(C_n - C)(H_n - H)^*(cHCH^* + tI)^{-\frac{1}{2}}\|_\infty \leq \frac{c}{t}\|H_n - H\|_\infty^2\|C_n - C\|_\infty$$

**[Bound (vii)]**

$$\|(cHCH^* + tI)^{-\frac{1}{2}}H(C_n - C)H^*(cHCH^* + tI)^{-\frac{1}{2}}\|_\infty \leq \frac{c}{t}R^2\|C_n - C\|_\infty$$

**[Conclusion]**

Hence, noting  $u_n = \frac{4\kappa^2 \log \frac{2}{\delta}}{\sqrt{n}}$ ,  $v_n = \mathbb{E}_x(\|\hat{h}(x) - h^*(x)\|^2)$ ,  $w_n = \frac{4Q\kappa \log \frac{2}{\delta}}{\lambda\sqrt{n}}(1 + \|h_\psi^*\|_{\mathcal{H}}) + \lambda\|h_\psi^*\|_{\mathcal{H}}$ , if  $t \geq 5 \max(4c^2v_n, 2cv_n, 4cRw_nu_n, 2cw_n^2u_n, 2R^2u_n)$ , by union bound with probability  $1 - 2\delta$

$$\|B_n\|_\infty \leq \frac{1}{2}$$

As, with probability  $1 - \delta$ :  $\|(C_n - C)\|_\infty \leq u_n$  (cf. [8], proof of lemma 18.), and also with probability  $1 - \delta$  (cf. lemma 6.6):  $\|H_n - H\|_\infty \leq w_n$ .  $\square$

### 6.3 Theorem

In this section we prove a stronger version of Theorem 3.3: Theorem 6.8 below, with a change of the reconstruction error term from  $\mathcal{O}(1/p^{(r-1)/4})$  to  $\mathcal{O}(1/p^{(r-1)/2})$  and better constants.

**ERRATUM.** Corollary 3.3.1 does not hold true, but 6.8.1 below holds.

**Theorem 6.8** (Excess-risk bound, KRR + linear OEL). *Let  $\rho$  be a distribution over  $\mathcal{X} \times \mathcal{Y}$ ,  $\rho_y$  the marginal of  $Y$ ,  $(x_i, y_i)_{i=1}^n$  be i.i.d samples from  $\rho$ ,  $(y_i)_{i=1}^m$  i.i.d samples from  $\rho_y$ ,  $\lambda \leq \kappa^2 := \sup_{x \in \mathcal{X}} \|k_x(x, \cdot)\|_{\mathcal{H}_x}$ ,  $\delta > 0$ , and  $M_c$  and  $h_\psi^*$  satisfy Assumption 1 and 2. When*

$$p^r \leq \min \left\{ \frac{\omega m}{9(1-c) \log(m/\delta)}, \frac{\omega}{8ct_n} \right\}, \quad (18)$$

then the following holds with probability at least  $1 - 4\delta$ ,

$$\sqrt{\mathbb{E}_x(\|\tilde{g} \circ \hat{h}_g(x) - h_\psi^*(x)\|^2)} \leq \underbrace{C \frac{Q+R}{\sqrt{\lambda n}} \log^2 \frac{10}{\delta} + R\sqrt{\lambda}}_{\text{KRR excess-risk on linear subspace of dimension } p} + \underbrace{\sqrt{\frac{\Omega'}{p^{r-1}}}}_{\text{Reconstruction error}},$$

where  $Q = \sup_{y \in \mathcal{Y}} \|k(y, \cdot)\|_{\mathcal{H}_y}$ ,  $R = \|h_\psi^*\|_{\mathcal{H}_x \times \mathcal{H}_y}$ ,  $C = 4\kappa(1 + (4\kappa^2/\sqrt{\lambda n})^{1/2})$ ,  $t_n = 5 \max(4c^2v_n, 2cv_n, 4cRw_nu_n, 2cw_n^2u_n, 2R^2u_n)$ , with  $u_n = \frac{4\kappa^2 \log \frac{2}{\delta}}{\sqrt{n}}$ ,  $v_n = \mathbb{E}_x(\|\hat{h}_\psi(x) - h_\psi^*\|^2)$ ,  $w_n = (\frac{Q}{\lambda\kappa}u_n(1+R) + \lambda R)$ . Finally  $\Omega' = \Omega_{q_r}$ ,  $q_r$  a constant depending only on  $r$  (defined in the proof).

*Proof.* First, we bound  $\mathbb{E}_x(\|\tilde{g} \circ \hat{h}_g(x) - h_\psi^*(x)\|^2)$  by decomposing it in two parts. We have, defining  $\hat{P} = \hat{G}^* \hat{G}$ ,

$$\mathbb{E}_x(\|\tilde{g} \circ \hat{h}_g(x) - h_\psi^*(x)\|^2) = \mathbb{E}_x(\|\hat{P}\hat{h}_\psi(x) - h_\psi^*(x)\|^2) \quad (19)$$

$$= \underbrace{\mathbb{E}_x(\|\hat{P}(\hat{h}_\psi(x) - h_\psi^*(x))\|^2)}_{(1)} + \underbrace{\mathbb{E}_x(\|\hat{P}h_\psi^*(x) - h_\psi^*(x)\|^2)}_{(2)} \quad (20)$$

We now bound the two terms of equations (19).

**[Bound (1) =  $\mathbb{E}_x(\|\hat{P}(\hat{h}_\psi(x) - h_\psi^*(x))\|^2)$ ]** We upper bound this term using Lemma 6.2.

**[Bound (2) =  $\mathbb{E}_x(\|\hat{P}h_\psi^*(x) - h_\psi^*(x)\|^2)$ ]** We upper bound this term using two dedicated lemmas, first Lemma 3.2, then Lemma 6.3, with  $t = \max(\sigma_k(N), t_1, t_2)$ . If  $p^r \leq \min(\omega/t_1, \omega/t_2^n)$ , then  $\sigma_k(N) \geq \max(t_1, t_2)$ , so  $t = \sigma_k(N)$ , and with probability  $1 - 3\delta$ :

$$\begin{aligned} \sqrt{\mathbb{E}_x(\|\hat{P}h_\psi^*(x) - h_\psi^*(x)\|^2)} &\leq \sqrt{\langle I - \hat{G}^* \hat{G}, M_c \rangle_{\mathcal{H}_y \otimes \mathcal{H}_y}} \\ &\leq 3\Omega' t^{-1/2r} \sqrt{2\sigma_k(N)} \\ &= 3\sqrt{2}\Omega' \sigma_k(N)^{1/2(1-1/r)} \\ &\leq \sqrt{\Omega_{q_r}} \times p^{(1-r)/2} \end{aligned}$$

with:  $q_r = 36 \times \Gamma(1 - 1/r)\Gamma(1 + 1/r)\Gamma(1/r)$

We conclude the desired bound by union bound.  $\square$

**Corollary 6.8.1.** *Under the same assumptions of Theorem 3.3, let  $\lambda = 1/\sqrt{n}$ . Then, running the proposed algorithm with a number of components*

$$p \gtrsim n^{\frac{1}{2r}},$$

*is enough to achieve an excess-risk of  $\mathcal{R}(\hat{f}) - \mathcal{R}(f^*) = O(n^{-(1-\frac{1}{r})/4})$ .*

*Proof.* We have:  $u_n = \mathcal{O}(n^{-1/2})$ , and using  $\lambda = 1/\sqrt{n}$ , we have  $v_n = \mathbb{E}_x(\|\hat{h}(x) - h^*(x)\|^2) = \mathcal{O}(n^{-1/2})$ , and  $w_n = \mathcal{O}(1)$ , so we can use a number of components  $p = \mathcal{O}(n^{-1/2r})$  and having the condition on  $p$  of the theorem verified:  $p^r \leq \min \left\{ \frac{\omega m}{9(1-c) \log(m/\delta)}, \frac{\omega}{8ct_n} \right\}$ .

Now, injecting  $p = \mathcal{O}(n^{-1/2})$  in the reconstruction error term we get the desired  $O(n^{-(r-1)/4r})$ .  $\square$

It's interesting to note that when  $r$  increases  $O(n^{-(r-1)/4r})$  becomes really close to the typical rate of  $O(n^{-1/4})$  but with a number of components  $p \ll n$ .

## 6.4 Additional Experimental Results and Details

### 6.4.1 Image Reconstruction

**Experimental setting.** As in [40] we used as target loss an rbf loss  $\|\psi(y) - \psi(y')\|^2$  induced by a Gaussian kernel  $k$  and visually chose the kernel's width  $\sigma_{output}^2 = 10$  looking at reconstructed images of IOKR without embedding learning. We constituted a supervised training set with the first 1000 train digits, and an unsupervised training set with the 6000 last bottom half train digits. We used a Gaussian input kernel of width  $\sigma_{input}$ . For the pre-image step, we used the same candidate set for all methods constituted with all the 7000 training bottom half digits. We selected the hyper-parameters  $\gamma_{input}, p, \lambda$  using logarithmic grids and the supervised/unsupervised balance parameter  $\gamma$  using linear grid, via 5 repeated random sub-sampling validation (80%/20%) selecting the best mean validation MSE, then we trained a model on the entire training set, and we tested on the test set.

**Link to downloadable dataset** [https://web.stanford.edu/~hastie/StatLearnSparsity\\_files/DATA/zipcode.htm](https://web.stanford.edu/~hastie/StatLearnSparsity_files/DATA/zipcode.htm)

### 6.4.2 Multi-label classification

**Problem and dataset** Bibtex and Bookmarks [18] are tag recommendation problems, in which the objective is to propose a relevant set of tags (e.g. url, description, journal volume) to users when they add a new Bookmark (webpage) or Bibtex entry to the social bookmarking system Bibsonomy. Corel5k is an image dataset and the goal of this application is to annotate these images with keywords. Information on these datasets is given in Table 4.

| Dataset   | $n$   | $n_{te}$ | $n_{features}$ | $n_{labels}$ | $\bar{l}$ |
|-----------|-------|----------|----------------|--------------|-----------|
| Bibtex    | 4880  | 2515     | 1836           | 159          | 2.40      |
| Bookmarks | 60000 | 27856    | 2150           | 208          | 2.03      |
| Corel5k   | 4500  | 499      | 37152          | 260          | 3.52      |

Table 4: Multi-label datasets description.  $\bar{l}$  denotes the averaged number of labels per point.

**Experimental setting** For all multi-label experiments we used a Gaussian output kernel with widths  $\sigma_{output}^2 = \frac{1}{\bar{l}}$ , where  $\bar{l}$  is the averaged number of labels per point. As candidate sets we used all the training output data. We measured the quality of predictions using example-based F1 score. We selected the hyper-parameters  $\lambda$  and  $p$  in logarithmic grids.

**Link to downloadable dataset** <http://mulan.sourceforge.net/datasets-mlc.html>

### 6.4.3 Metabolite identification

**Problem and dataset** An important problem in metabolomics is to identify the small molecules, called metabolites, that are present in a biological sample. Mass spectrometry is a widespread method to extract distinctive features from a biological sample in the form of a tandem mass (MS/MS) spectrum. In output the molecular structures of the metabolites are represented by fingerprints, that are binary vectors of length  $d = 7593$ . Each value of the fingerprint indicates the presence or absence of a certain molecular property. Labeled data are expensive to obtain, but a very large unsupervised dataset (several millions, 6455532 in our case) is available in output. For each input the molecular formula of the output is assumed to be known, and we consider all the molecular structures having the same molecular formula as the corresponding candidate set. The median size of the candidate sets is 292, and the biggest candidate set is of size 36918.

**Experimental setting** The dataset contains 6974 supervised data  $(x_i, y_i)$  and several millions of unlabeled data are available in output. In input we use a probability product kernel on the tandem mass spectra. As output kernel we used a Gaussian kernel (with parameter  $\sigma^2 = 1$ ) in which the distances are taken between feature vectors associated with a Tanimoto kernel. When no additional unsupervised data are used, we selected the hyper-parameters  $\lambda, p$  in logarithmic grids using nested cross-validation with 5 outer folds and 4 inner folds. In the case of OEL with  $10^5$  additional unsupervised data, we fixed  $p = 2000$ , and selected  $\lambda, \gamma$  with 5 outer folds and 4 inner folds but only using  $5 \times 10^3$  additional data.

### 6.5 Label Ranking

The goal of label ranking is to learn to rank  $K$  items indexed by  $1, \dots, K$ . A ranking can be seen as a permutation, i.e a bijection  $\sigma : [1, K] \rightarrow [1, K]$  mapping each item to its rank.  $i$  is preferred over  $j$  according to  $\sigma$  if and only if  $i$  is ranked lower than  $j$ :  $\sigma(i) < \sigma(j)$ . The set of all permutations over  $K$  items is the symmetric group which we denote by  $S_K$ , and can be seen as a structured objects set (cf. [19]).

[19] have shown that IOKR is a competitive method with state of the art label ranking methods. We evaluate the performance of OEL on benchmark label ranking datasets. Following [19] we embedded the permutation using Kemeny embedding. We trained regressors using Kernel ridge regression (Gaussian kernel). We adopt the same setting as [19] and report the results of our predictors in terms of mean Kendall’s  $\tau$  from five repetitions of a ten-fold cross-validation (c.v.). We also report the standard deviation of the resulting scores. The parameters of our regressors and output embeddings learning algorithms were tuned in a five folds inner c.v. for each training set.

The results are given in Table 5. Learning a linear output embedding from Kemeny embedding shows a small improvement in term of Kendall’s  $\tau$  compared to IOKR. This improvement is observed on all the datasets.

| Method           | cold                                | diau                                | dtb                                 | heat                                |
|------------------|-------------------------------------|-------------------------------------|-------------------------------------|-------------------------------------|
| IOKR             | $0.097 \pm 0.033$                   | $0.228 \pm 0.023$                   | $0.135 \pm 0.036$                   | $0.058 \pm 0.020$                   |
| OEL <sup>0</sup> | $0.097 \pm 0.034$                   | $0.228 \pm 0.026$                   | <b><math>0.136 \pm 0.036</math></b> | <b><math>0.059 \pm 0.022</math></b> |
| OEL <sup>1</sup> | <b><math>0.105 \pm 0.029</math></b> | <b><math>0.231 \pm 0.026</math></b> | $0.132 \pm 0.036$                   | $0.056 \pm 0.021$                   |
| sushi            |                                     |                                     |                                     |                                     |
| IOKR             | $0.321 \pm 0.021$                   |                                     |                                     |                                     |
| OEL <sup>0</sup> | <b><math>0.326 \pm 0.023</math></b> |                                     |                                     |                                     |
| OEL <sup>1</sup> | $0.325 \pm 0.027$                   |                                     |                                     |                                     |

Table 5: Mean Kendall’s  $\tau$  coefficient (higher is better) obtained with IOKR and OEL methods on several label ranking datasets.

## 6.6 Analysis of the Time and Space Complexities of Algorithm 1

**Train.** The algorithm 1 consists, during the training phase, in training an estimator of the output embedding thanks to a kernel ridge regression and a singular value decomposition of the output kernel matrix. The complexities of algorithm 1 are given by summing the complexities of the two steps. We give in Tables 6 and 7 the time and space complexities for these latter. Both can be solved using standard approximation methods, and we give the complexity of algorithm 1 when using Nyström KRR approximation of rank  $q$  and randomized svd approximation of rank  $p$ .

**Test.** The algorithm 1 consists, during the test phase, in a kernel ridge prediction of the output embedding and a prediction of the structured object through a decoding (k-nearest neighbors). The decoding part is computationally very expensive, in general, as it requires an exhaustive search in the candidate sets which can be very large.

| Algorithm    | KRR                       | SVD                                |
|--------------|---------------------------|------------------------------------|
| Standard     | $\mathcal{O}(n^3)$        | $\mathcal{O}((n+m)^3)$             |
| Approximated | $\mathcal{O}(nq^2 + q^3)$ | $\mathcal{O}((n+m)^2p + (n+m)p^2)$ |

Table 6: Training time complexity of algorithm 1

| Algorithm    | KRR                     | SVD                    |
|--------------|-------------------------|------------------------|
| Standard     | $\mathcal{O}(n^2)$      | $\mathcal{O}((n+m)^2)$ |
| Approximated | $\mathcal{O}(q^2 + nq)$ | $\mathcal{O}((n+m)p)$  |

Table 7: Training space complexity of algorithm 1